Proc. 8th NZ Ceothermal Workshop 1986

# SIMULATION OF THE TONGONAN GEOTHERMAL FIELD THE INITIAL STATE : PRELIMINARY RESULT

Z.P. Aunzo, Z.F. Sarmiento and A.D. Sarit

PNOC–Energy Development Corporation

## ABSTRACT

The Tongonan geothermal field is conceptualized in a three–dimensional three–layered model. The model covers 5.4 x 3.0 km of the field and is 800m thick.

A steady–state simulation was run to approximate the pre–exploitation condition of the Tongonan reservoir. Comparison of the simulation results with observed field pressures, temperatures and enthalpies produced a good match. Estimated permeabilities in the reservoir range from 5 to 100 md in the horizontal, and 0.05 to 5 md in the vertical directions. A natural upflow of 25 kg/s is also estimated near the Sambaloran/Upper Mahiao area.

With the completion of the steady–state simulation of the field, modelling of its response to exploitation may now proceed.

## INTRODUCTION

The natural state of a geothermal system is the undisturbed state of the reservoir describing the characteristics of the system prior to production. Although a geothermal system is complex and dynamic, the changes that occur are considered insignificant when compared to the effects of exploitation over a short period of time. Thus, it is inferred that the natural state of many known geothermal systems can be considered as a steady state system.

It is the intention of this study to approximate the natural state of the Tongonan Geothermal Field (TGF) in preparation for the modelling of its response to exploitation. Towards this goal, analyses of fluid and rock properties derived from well tests and geoscientific investigations were done. The resulting natural state model of the field was then checked against the current state of the reservoir by simulation, as Bodvarsson et. al. (1985) state that simulation is the only way in which a consistent set of initial and boundary conditions for exploitation models can be developed.

## FIELD DESCRIPTION

The Tongonan geothermal reservoir is generally liquid–dominated, with a two–phase zone lying above a single–phase liquid at the bottom of the reservoir. Vapor–dominated fluids are mainly observed in the Mahiao and Sambaloran sectors. At the central uppermost portion of the reservoir, evidences for the formation of a steam cap have been manifested in the discharges of wells 209 and 208. In the South Sambaloran and Malitbog sectors, boiling is also interpreted as occurring in the upper part of the reservoir with undersaturated liquid at the bottom. In some wells, the shape of the temperature profiles follows the boiling-point-for–depth curve.

The temperature distribution in the area indicates that the hottest portion in the field is situated within the vicinity of wells 410, 209 and 401, over the same area where the Mahiao Pluton is located. Figure 1 shows the temperature contour as developed by Aunzo (1983). The maximum temperature ever recorded is 339°C at well 410, although the highest temperature is suspected to be at well 209A (>350°C) (Stock and Sarit, 1983). Well 209A penetrated the Mahiao Pluton, considered as part of the heat source of the system, but was later blocked by undetermined causes. The temperature decreases gradually from the north to the south and down to the Bao Valley, indicating lateral flow and fluid dilution.

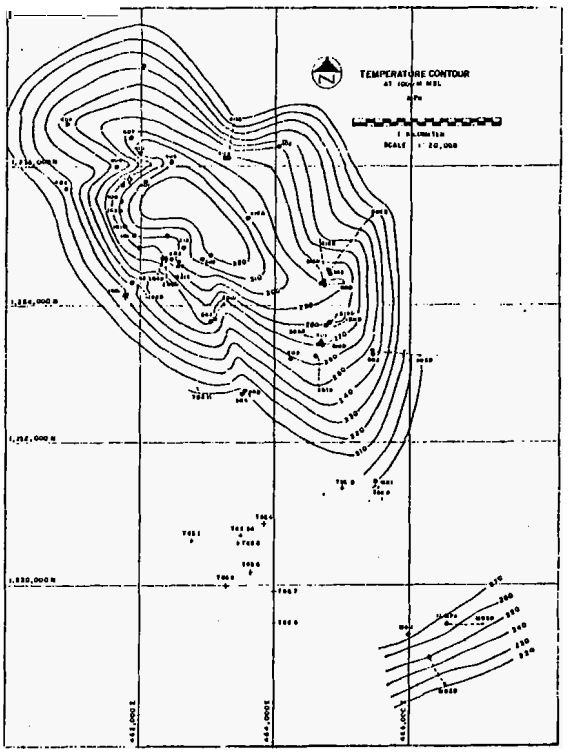


Figure 1. Temperatures at -1000m MSL.

In Mahiao and Sambaloran wells, temperature profiles are indicative of fluid upflows. These are most visible at 406, 410, 401, 407, 404, 212, 214 and 209A. Temperature reversals exist towards the north at well 405, towards the east at wells 502 and 506D, and towards the south as first noted at well 214. These persist in the direction of 303 and 504, confirming the strong horizontal fluid flow towards the Malitbog and Bao hot springs, and the large horizontal permeability in such direction.

Farther to the south in the Mahanagdong area, three more wells encountered temperatures of 270–310°C. These wells were sited several kilometers

away from Malitbog, and farther south of the comparatively tight and dry Mamban area. The possibility, therefore, that Mahanagdong is supplied by a source other than Mahiao is unambiguous.

High pressures (Sarit, 1983) were measured in the Mahiao sector, about the location of the upwelling zone (Figure 2). The pressure decreases gradually towards the direction of wells 402, 403, 405, 502, 504 and 505D. The contours also indicate a separate pattern in the Mahanagdong area, supplementing the findings from the temperature data.

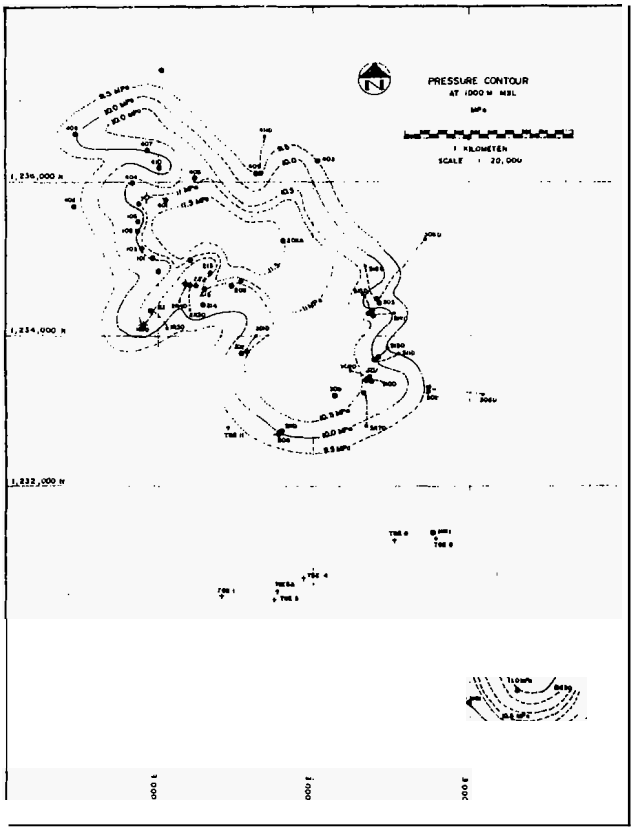


Figure 2. Pressure Contour at -1000m MSL.

Well output characteristics generally reflect mixed contribution coming from two-phase and single-phase feed sources. The main feature of the discharges in Mahiao and Sambaloran is that at full bore discharge (FBD) condition the high-enthalpy upper production zone dominates. On the other hand, at choked condition, the wells are dominantly fed by the lower zone which is single-phase. Wells in the Malitbog and Mahanagdong sectors are basically wellbore-controlled. In contrast, wells in Mahiao are formation-controlled.

Permeability in many wells were initially encountered at about -300m MSL, though occasional drilling losses were intercepted above this level. In the Mahiao sector, this level is part of the upper two-phase zone which extends from -300m to -500m. The degree of permeability, however, encountered in this interval is not sufficient to sustain a prolonged discharge, much more a large-scale exploitation. Below this upper zone, i.e., from -600 to -1200m, clusters of permeable zones were located, especially at -900 to -1100m. This zone corresponds to the contact between the overlying volcanics and the Mahiao Pluton. It has been deduced by several authors that this zone acts as the major channel of geothermal fluids in the system.

## CONCEPTUAL MODEL

Based on the foregoing data interpretation, a conceptual model of the field which forms the basis for subsequent simulation was established. The upwelling zone has been described to be located in the central part of the Mahiao and Sambaloran sector. Chemical interpretation indicates that the source fluid flow rate may range from 35 to 100 kg/s. Fluid flows preferentially to the south via Malitbog to the Bao Valley. Another outflow is deduced in the north through well 405 as indicated by temperature reversals. Figure 3 shows the hydrological flow model of Lovelock et al (1982). At the top of the reservoir, a steam cap is believed to be present as recognized in wells 208 and 209. Wells tapping this part of the reservoir produce high-enthalpy fluids. The reservoir is bounded by low-permeability young volcanics at the top and by the Mahiao plutonic complex below. Maximum permeability is found at the contact of the pluton and the overlying altered volcanics.

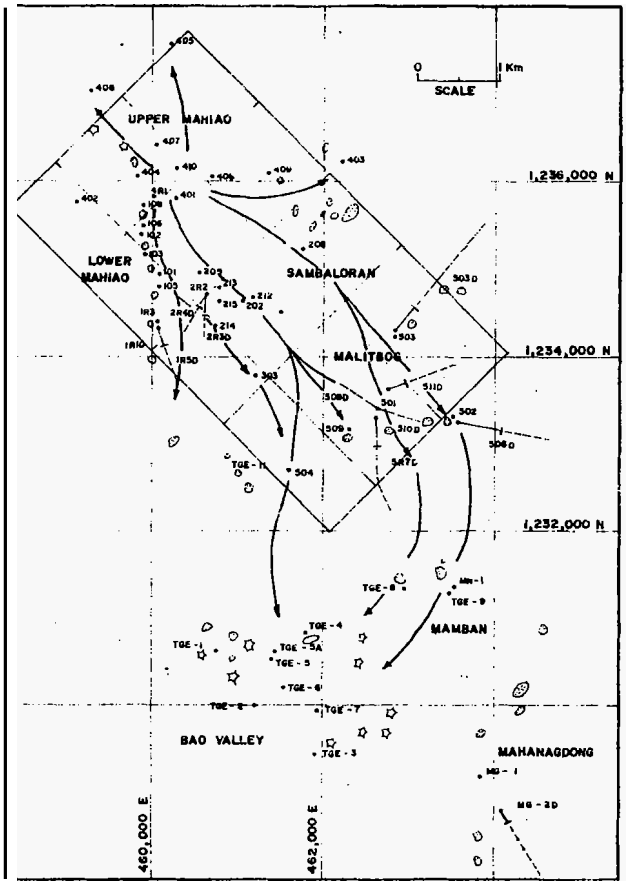


Figure 3. Hydrological Flow Model.

Figure 4 shms the integrated model of the field.

## SIMULATION MODEL

The model used for the simulation work was built to provide answers associated with the development and exploitation of the whole Tongonan field, including Tongonan I, II and III. A rectangular atea measuring 5.4 x 3.0 km (16.2 $km^2$) and encompassing the Mahiao, Sambaloran and Malitbog sectors was blocked for the model. The geometrical shape of the model was based on the temperature and pressure distribution, hydrological flow model and the geologic structures which run across the field. The Mahanagdang sector is not part of the model since it is postulated to be connected to a different

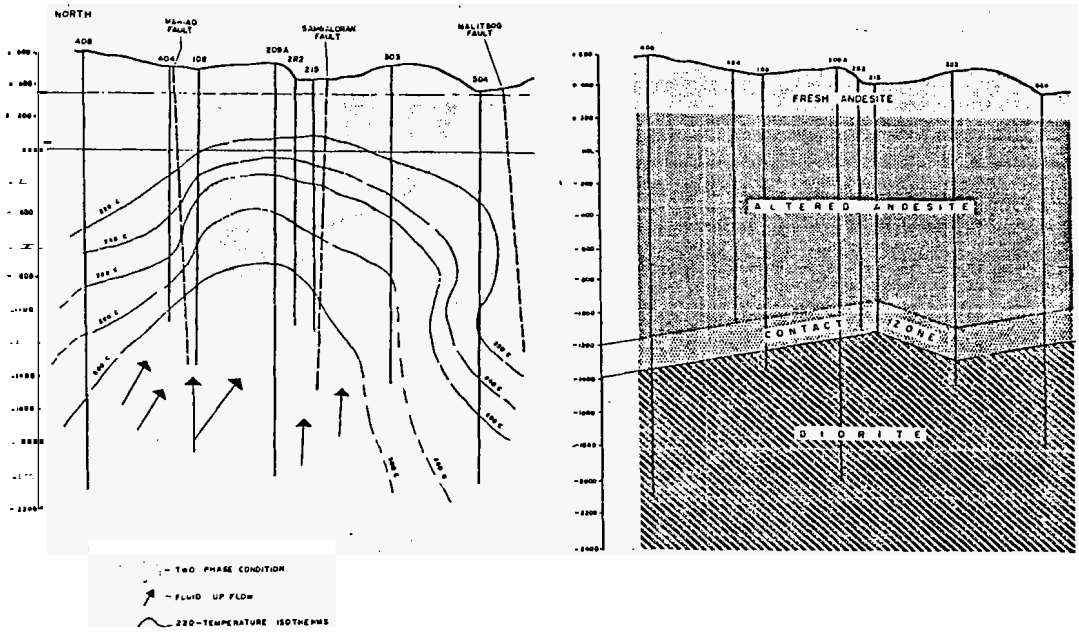


Fig. 4. Conceptual Model of the Field.

system. Consequently, the concentration of the work was focused on the Mahiao and Sambaloran sectors from where the 112.5-MWe Tongonan I power station draws its steam supply.

The following considerations were used in framing up the field geometry.

(1) Separate the deduced upflow from the outflow region.

(2) Isolate the inferred two-phase zone from the single-phase region.

(3) Lump, as much as possible, the wells with the same characteristics into a single block..

(4) Separate, if possible, the reinjection wells from the production wells.

(5) Segregate the permeable zones found at various levels.

The simulation uses a geometry of 3 x 4 x 3 grids (Figure 5). The thickness of the reservoir is based on the distribution of the permeable zones encountered in each well. The top of the main reservoir is at -300m MSL while the base is at -1100m MSL. However, the reservoir basement may actually extend deeper than -1100m. The interval where the contact zone was found is also at this junction. As described in the reservoir model, there exist the upper and the lower zones. The upper zone is inferred to be from -300m to -500m MSL, while the lower zone extends from -900m -1100m. Based on this, the reservoir is divided into 3 layers; layer 3 at -300m to -500m, layer 2 at -500 to -900m and layer 1 from -900 to -1100m. The middle layer (layer 2) is relatively impervious compared to the other two layers. Some wells, however, produce at this level.

All other parameters like the boundary conditions, mass sources and sinks. two-phase region and temperatures and pressures were taken from the conceptual model.

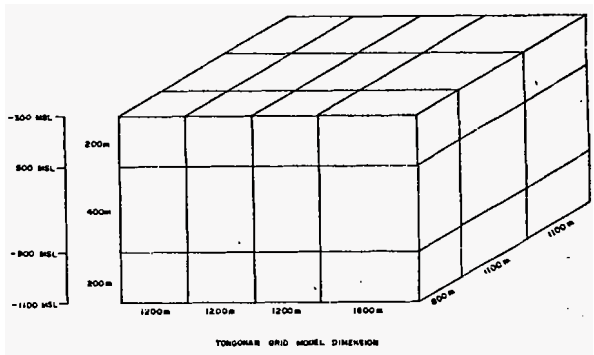


Fig. 5. Grid Block Dimensions and Well Locations.

## APPROACH TO SIMULATION WORK

The simulation work was done by calibrating the pre-production state through forward simulation until a steady state condition of the system was reached. The whole process involved trial-and-error adjustments of various parameters like upflow rate and enthalpy, steam saturation, vertical and horizontal permeabilities, and location of mass sources and sinks. Other parameters which were considered undefinable were treated less frequently as studies showed they were less likely to cause significant changes in the reservoir. Some of these parameters include porosity, rock expansibility, compressibility, rock density and heat capacity.

All input data were based on available geoscientific, well test and measurement data. Rock distribution throughout the field was deduced by correlating all data obtained from cores and cuttings. Rock properties were obtained from tables in published literatures. The rock permeability values were derived from the analysis of well test data. Single well test results show significantly

| Rock Type | Name | Heat Capacity J/kg-°C | Conductivity W/m-°C | Density kg/m³ | Initial Porosity | Permeability x $10^{-15}$ m² x | y | z | Coeff of Linear Expansion Rock Grain | Dry Rock | Bulk Modulus Loading | Unloading | Shear Modulus |
|---|---|---|---|---|---|---|---|---|---|---|---|---|---|
| 1 | ANDESITE 1 | 685 | 1.39 | 2520 | 0.10 | 3.0 | 3.0 | 0.03 | 5.0E-6 | 5.0E-6 | 3.0E10 | 3.0E10 | 2.3E10 |
| 2 | ANDESITE 2 | 685 | 1.39 | 2520 | 0.10 | 2.0 | 2.0 | 0.02 | 5.0E-6 | 5.0E-6 | 3.0E10 | 3.0E10 | 2.3E10 |
| 3 | ANDESITE 3 | 685 | 1139 | 2520 | 0.10 | 1.0 | 1.0 | 0.20 | 5.0E-6 | 5.0E-6 | 3.0E10 | 3.0E10 | 2.3E10 |
| 4 | ANDESITE 4 | 685 | 1.39 | 2520 | 0.10 | 1.0 | 1.0 | 0.01 | 5.0E-6 | 5.0E-6 | 3.0E10 | 3.0E10 | 2.3E10 |
| 5 | ANDESITE 5 | 685 | 1.39 | 2520 | 0.10 | 5.0 | 5.0 | 0.05 | 5.0E-6 | 5.0E-6 | 3.0E10 | 3.0E10 | 2.3E10 |
| 6 | CONTACT ZONE 1 | 668 | 1.67 | 2620 | 0.06 | 20.0 | 10.0 | 0.10 | 6.0E-6 | 6.0E-6 | 3.5E10 | 3.5E10 | 2.7E10 |
| 7 | CONTACT ZONE 2 | 668 | 1.67 | 2620 | 0.06 | 10.0 | 5.0 | 0.05 | 6.0E-6 | 6.0E-6 | 3.5E10 | 3.5E10 | 2.7E10 |
| 8 | CONTACT ZONE 3 | 668 | 1.67 | 2620 | 0.06 | 10.0 | 5.0 | 1.00 | 6.0E-6 | 6.0E-6 | 3.5E10 | 3.5E10 | 2.7E10 |

Table 1. Rock Types and Properties

lower permeabilities (1 to 10 md) than interference test results (10 to 160 md) in Malitbog (Sarmiento et. al., 1984). The results of interference tests are considered more applicable and, therefore, were used as the main basis for permeability adjustments. It is estimated that the reservoir permeability may be in the range of 10 to 200 millidarcies.

Two methods were employed, as provided by the simulator, to specify the fluid thermodynamic conditions. For single-phase liquid, parameters used where temperature and pressure. However, for the two-phase region, density and internal energy were taken at the center of the block, using the temperature contours discussed in the preceding sections. Pressures in the single-phase zones were based on the average pressure gradient of the field (0.8 MPa/100 m) and the inferred piezometric level (Sarit, 1983). On the other hand, internal energy and density in the two-phase zones were based on all well discharges.

Initial values used for the natural flows were based on the natural discharges estimated from Bao Springs and other areas.

## BEST MODEL

Three models (Figure 6), which describe the outflow directions of the field, were initially considered. In setting up these models, the most prominent flow paths were inferred based on correlated data from temperature and pressure contours and the hydrological flow model.

The model which best fits the interpreted data has two prominent outflows: one towards the Bao valley (sink at block 413), and another towards the vicinity of well 405 (sink at block 133). A constant rate of 25 kg/s is specified for the postulated upflow at a temperature of 320°C. The outflow towards the Bao valley is estimated at 20 kg/s, while another 5 kg/s flows towards well 405. Comparison between the initial input data and run results is discussed in detail in a related report (PNOC-EDC, 1986).

Only two lithologic units cover the field in the simulation model; one is Andesite and the other is a hybrid lithology at the contact of the Mahiao Pluton and the overlying Andesite. For simplicity. the latter has been named "Contact Zone" in this study. Variations in the physical properties of these lithologies resulted to eight differing rock types. Table 1 has the physical rock properties used in the model.

The permeability distribution shows increasing trend towards the Malitbog area. Furthermore, permeability was found to be mainly controlled by lithology. Simulation results shcw the permeability in the Contact Zone to be ten times larger than that of the Andesite. The values found for the Tongonan field are in the range of 5-100 md and are consistent with the results of interference tests. The spatial permeability distribution in the field has been expressed in ratios, and is summarized in Table 2.

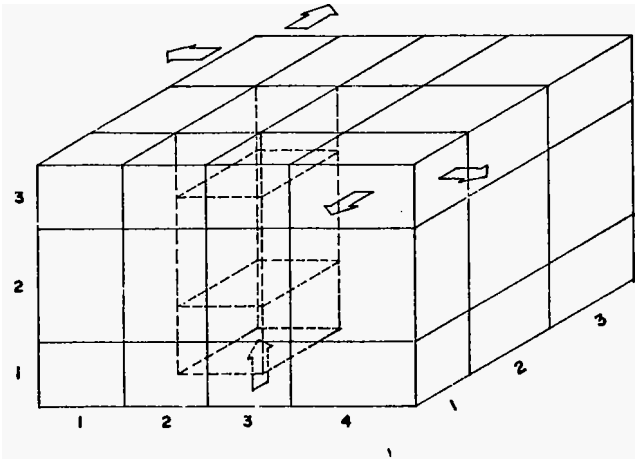


Figure 6. The Tongonan Flow Model.

| ROCK TYPE | NAME | X:Y:Z: RATIO |
|---|---|---|
| 1 | Andesite 1 | 100: 100: 1 |
| 2 | Andesite 2 | 100:100:1 |
| 3 | Andesite 3 | 5: 5:1 |
| 4 | Andesite 4 | 100:100:1 |
| 5 | Andesite 5 | 100: 100:1 |
| 6 | Contact Zone 1 | 200: 100:1 |
| 7 | Contact Zone 2 | 200:100:1 |
| 8 | Contact Zone 3 | 10: 5:1 |

Table 2. Permeability Ratios.

The model reservoir has impermeable but conductive top and bottom layers. Constant pressure boundaries are specified at the sides to permit lateral flows. The pressures specified at the boundaries, however, are the same as the connecting grid blocks.

Straight line relative permeability function is assumed with irreducible liquid and vapor saturations of 0.5 and 0 respectively.

## SENSITIVITY STUDIES

In order to investigate the effect of various parameters, changes were made on the type and flowrate of the source, permeability distribution and boundary conditions.

The model of the Tongonan reservoir uses a permeability distribution which takes into account the inferred upflow. In order to investigate the effect of this parameter, changes in the distribution along the upflow region were made. In this case, permeabilities along the x and y directions were held constant. However, permeability ratios along the upflow were identical with the surrounding blocks. This situation, in effect, decreases the permeability along the $z$ axis. Results showed that more fluid moves laterally along layer 1 and less up the top layer. Temperatures were generally found to be much higher in the bottom layer and lower in the upper two layers. As a result, the inferred two-phase region was not matched. Only two blocks (223 and 323) showed two-phase conditions.

In order to test the uniqueness of the model assuming a dynamic system, a run was made using only conductive heat as the source instead of a mass source. The heat source specified had an equivalent content of a 320°C fluid at 25 kg/s. The result did not produce a good match with the observed field temperatures. Unrealistic high values were obtained at the upflow blocks. An additional run was conducted in an attempt to check the accuracy of the specified upflow. In this case, the sources and sinks were reduced 5 times. Furthermore, the permeability values were reduced by the same magnitude although the same ratios were maintained. The run showed good match in temperature and pressure, However, the inferred steam cap at the uppermost layer was not reproduced. The two-phase region was only limited to one block, 223.

In the best model chosen, constant pressure boundaries at the sides were specified to provide for fluid transport. This parameter, though not very significant during the initial state, would become very important during the exploitation stage. A constant pressure boundary would serve as a channel for cold water influx as the field draws down.

Two sensitivity runs were conducted to check the boundary conditions specified. In the first run, constant boundary pressures which were lower than those at the reservoir grid blocks were specified. Temperatures showed good match. However, a uniform decrease in pressure was observed for the three layers. All the blocks decreased to a value equal to the pressure of the boundaries.

Another run was done assuming a closed system, i.e., impermeable but conductive boundaries enclosing the reservoir. Both temperature and pressure did not produce a good match with the observed values. Pressures in the reservoir rose to values of more than 20 MPa. The temperature, likewise, rose by a maximum of about 40°C in the upflow region. Also, the inferred two-phase region in the top layer was not reproduced as single-phase fluid occupied the entire layer.

## CONCLUSION

A three-dimensional model that reproduces the temperature and pressure distribution of the field was developed. The following conclusions can be drawn from this work:

(1) The Tongonan Geothermal Field is a dynamic system and an upflow exists beneath the Mahiao/Sambaloran area.

(2) The hydrological flow model is consistent with the mass and heat flow of the reservoir.

(3) The upflow is found to be at a temperature of 320°C and the flow rate is about 25 kg/s. The hot water plume boils as it ascends and produces a steam cap at the upper part of the reservoir.

(4) Reservoir permeability is mainly controlled by lithology. Horizontal permeability values were found to be in the range of 5–100 md and the vertical permeability between .05–5 md. Higher permeabilities were determined in the Malitbog area.

(5) Lower permeabilities exist at the top and bottom layers of the reservoir. Side boundaries, however, were found to provide fluid flows.

## ACKNOWLEDGMENT

The authors wish to thank their colleagues for the support, and the management of the Philippine National Oil Company - Energy Development Corporation (Geothermal Division) for permission to publish this paper. Special thanks are also extended to Dr. Valgardur Stefansson of UNDP, Dr. Subir Sanyal of Geothermex and Dr. Malcolm Grant of DSIR for the fruitful discussions and advices.

## REFERENCES

Aunzo, Z.P. (1983). An Update of Tongonan Geothermal Field Temperature Contours (September, 1983). PNOC–EDC Internal Report.

Bodvarsson, G.S., Pruess, K., Stefansson, V., Bjornsson, S. and Ojiambo, S.B. (1985). A Summary of Modelling Studies of the East Olkaria Geothermal Field, Kenya. 1985 International Volume, Geothermal Resources Council, pp. 295–301.

Bodvarsson, G.S., Pruess, K., Stefansson, V., and Eliasson, E.T. (1984). The Krafla Geothermal Field, Iceland: 2. The Natural State of the System. Water Resources Research, Vol. 20, No. 11, pp. 1531–1544.

Castañeda, M., Marquez, R., Arellano, V. and Esquer, C.A. (1983). Reservoir Simulation on the Cerro Prieto Geothermal Field: A Continuing Study. Proceedings, 9th Workshop on Geothermal Reservoir Engineering, Stanford University, Stanford, California.

Grant, M.A. (1983). Review No. 1 Geothermal Reservoir Modelling. Geothermics, Vol. 12, No. 4, pp. 351–363.

Grant, M.A., Garg, S.K. and Riney, T.D. (1984). Interpretation of Downhole Data and Development of a Conceptual Model for the Redondo Creek Area of the Baca Geothermal Field. Water Resources Researches, Vol. 10, No. 10, pp. 1401–1416.

Sarit, A.D. (1983). Reservoir Pressure in the Tongonan Geothermal Field (January 1977 - May 1983). PNOC–EDC Internal Report.

Sarmiento, Z.F., Aquino B.C. and Menzies, A.J. (1984). Analysis of the Interference Tests from the Malitbog Sector, Tongonan Geothermal Field, Republic of the Philippines. Proceedings, Sixth New Zealand Geothermal Workshop, pp. 163-167.

Sarmiento, Z.F. Sarit, A.D. and Salera, J. M. (1985). Response of the Production and Reinjection Wells During the Initial Exploitation of the Tongonan Geothermal Field, Philippines. Proceedings of the Seventh New Zealand Geothermal Workshop.

Stock, D.D. and Sarit, A.D. (1983). Prediction of Formation Temperature from the Early Heat-up Temperature Surveys. PNOC-EDC Internal Report.

PNOC-EDC (1986). The Tongonan Geothermal Reservoir. Report to UN/DTCD for UNDP Project PHI 80/014.